Pattern-formation characteristics of interacting kinematic waves

Michael Leibig*
Höchstleistungsrechenzentrum, Kernforschungsanlage Jülich G.m.b.H., Postfach 1913, 52425 Jülich, Germany
(Received 19 July 1993)

This work presents a model for the formation of density patterns in certain one-dimensional systems where the particle flux is a well-defined function of particle density (e.g., traffic flow or granular flow in a tube). In these systems, macroscopic regions characterized by large density contrasts are observed to evolve from very small-scale fluctuations. This paper shows that such patterns develop naturally when the small-scale noise is viewed as a set of stable density regions which propagate according to the formalism of kinematic waves. In the theory of kinematic waves, the interface separating a region of density ρ_1 from a region of density ρ_2 moves with a velocity $v=[j(\rho_1)-j(\rho_2)]/(\rho_1-\rho_2)$, where $j(\rho)$ is the flux at density ρ. With interfaces propagating according to this equation, both analytic and numerical results indicate that the noisy state is quickly replaced by a state in which neighboring density regions have a very large density contrast. Thus interacting kinematic waves and small-scale fluctuations are all that is necessary for this pattern formation.

PACS number(s): 05.40.+j, 05.60.+w, 46.10.+z, 89.40.+k

I. INTRODUCTION

One of the most universal experiences of modern life is sitting in traffic. It happens all over the world, and many researches have undertaken the study of this problem in order to understand the basic mechanism behind this phenomenon [1,2]. Among the numerous models for traffic flow, the one of most relevance to this study is a recent cellular automation model which is able to produce complex traffic patterns from a simple set of rules for driver behavior [2]. One of the key ingredients for the formation of these patterns is the presence of noise in the system, which can come in the form of disorder in the initial automobile positions, or through random "braking" events. In either case, this automaton produces very complicated traffic patterns which always possess regions of high traffic flow and regions with traffic jams.

A related problem, but one which is not such a part of everyday life, is the formation of density patterns in the flow of granular materials. When sand flows down a long tube, a spontaneous density pattern appears with regions of very high density in which the grains move very slowly, and low-density regions in which the velocity of the individual grains is very fast [3]. This pattern can be seen to move up or down, depending on experimental conditions. Similar patterns were also reported in the flow of granular materials through a hopper (i.e., a tube narrower at the bottom than the top) [4]. Numerical simulation of these two geometries using the techniques of molecular dynamics have been able to reproduce this behavior [3,5,6].

For the traffic problem, the theory of kinematic waves is able to explain the behavior of a single traffic jam moving in a uniform density background [7]. This theory is driven by the observation that in certain one-dimensional systems, there is a well-defined relationship between the flux, $j(x)$, at a point x, and the local density, $\rho(x)$ [i.e., $j(x)=j(\rho(x))$]. The continuity equation,

$$\partial_t \rho(x)+\nabla j(x)=0 , \tag{1.1}$$

then requires that the front which separates two regions of differing densities propagates with a well-defined velocity, v_f. The velocity for a front which separates a region with density ρ_1 from a region of density ρ_2 is given by the equation

$$v_f=\frac{j(\rho_1)-j(\rho_2)}{\rho_1-\rho_2} , \tag{1.2}$$

where $j(\rho)$ is the flux, or throughput, for the density ρ. Thus the propagation of the jammed regions is completely determined by the flux curve $j(\rho)$ for traffic flow.

In order to use kinematic wave theory to understand the density pattern in a granular system, there must be a well-defined $j(\rho)$ for the granular flow. In recent work by Lee, this curve has been measured using molecular-dynamics techniques which simulate the flow of spherical particles down a narrow tube [6]. He was also able to show that the velocity of these propagating fronts is given by Eq. (1.2).

The observation in both traffic and granular flow is that these systems evolve into a state in which high-density and low-density regions exist side by side, and that such density patterns travel coherently for some time. In both systems, these patterns begin as fluctuations at small length scales. This paper presents a possible mechanism by which these microscopic fluctuations evolve into the observed large-scale density patterns.

The basic idea behind this work is that if these small-

*Present address: Institute for Theoretical Physics, University of California, Santa Barbara, CA 93106.

scale density fluctuations are treated in the same manner as the large-scale perturbations [i.e., as density regions with stable interfaces which move according to Eq. (1.2)], then the system will naturally evolve to a state in which the density contrast between adjacent regions is, on average, as large as the largest fluctuations present in the original noise. Thus it is the interacting kinematic waves that produces the observed pattern. This view is in contrast to the idea that the density pattern results from some solution of the dynamic equation of motion.

The distinction between "dynamic" waves and kinematic waves is very subtle. This question is treated in some detail in the original work on kinematic waves by Lighthill and Whitham [7], and is also discussed by Lee [6]. The most important property of the kinematic wave approach is that the constraint of mass conservation, along with the flux curve $j(\rho)$, is all that is needed to determine the motion of an interface.

Another useful feature of the kinematic approach comes from the fact that many times the equation of motion can be very difficult to determine, while the flux curve can be measured or calculated with relative ease. This is certainly the case for sand flowing through a tube, and for traffic flow.

One of the basic assumptions in this work is that well-defined fronts exist which separate regions of different densities, and that such fronts are stable in time. This, in general, is not true. In the original paper on kinematic waves, it was shown that for the case of a traffic jam, the back of the jam quickly forms into a well-defined shock [7]. The leading edge, on the other hand, is shown to diffuse and this diffusion dissipates the entire jam at long times. Thus the results shown here may not properly describe the evolution at long times. However, at short times this approach should describe the essential behavior.

Additionally, there may be some properties of the system dynamics which do indeed act to stabilize these fronts. In the case of the cellular automation model for traffic flow, the nature of the acceleration rules for each car fixes the length scale over which the transition from a high-density to a low-density region occurs. Thus the assumption of well-defined fronts is valid at sufficiently large length scales.

The model system that is studied here is simple. Place N_0 points at random on an interval of length L. To each of the region between two successive points assign a density ρ_i. This density is taken from a uniform distribution in the range $[\rho_0-W,\rho_0+W]$. Each point then represents an interface between two density regions. The velocity of each interface is determined by (1.2), and it is a simple matter to propagate the interfaces forward in time, observing the evolution of the system. Figure 1 shows this schematically, and indicates how a density region can be "swallowed up" by its nearest neighbors. In this approach, no additional interfaces are ever created, and the density in a region can never become larger or smaller than any of the densities initially present. Because Eq. (1.2) is derived from the continuity equation, the mass of the system is conserved at all times during the evolution. Thus, if a density region is lost, this means

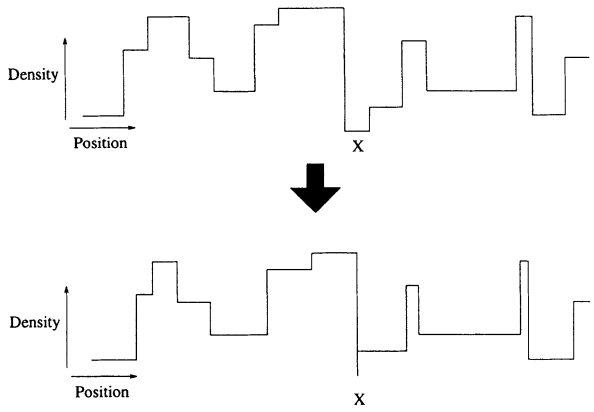

FIG. 1. Schematic representation of the evolution of a density pattern. In going from the upper configuration to the lower one, the region labeled X is "swallowed up" by its neighbors.

that all of the mass has simply been redistributed to its neighbors.

The principal numerical results of this paper are as follows. At early times, the number of interfaces decreases at a constant rate. As the number of interfaces is decreased, a correlated state is created in which the density pattern is "striped" in the sense that only those interfaces remain that separate regions which have large density contrasts (see Fig. 2). Once this state is reached, the behavior changes radically—the number of interfaces begins to decrease as a power law in time.

The evolution to the striped state can be understood from a relatively simple calculation which gives the evolution of the system at early times. The long-time power-law behavior is, however, much more problematic. The principle difficulty in understanding this evolution lies in the characterization of the striped density state.

The rest of this paper is organized in the following manner. In Sec. II, there is a discussion of the elementa-

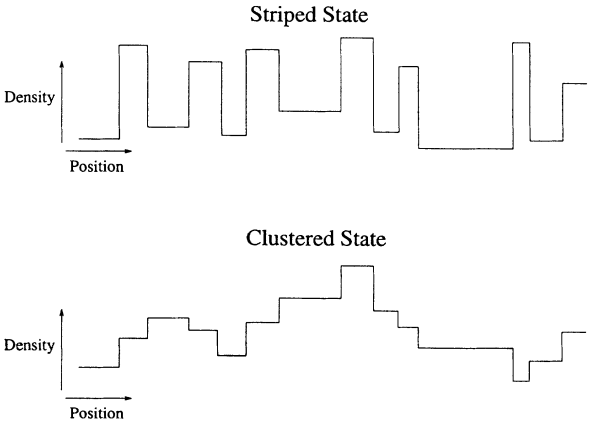

FIG. 2. Representation of a striped state. The density contrast between neighboring region is of the same order as the overall range of densities in the system. The lower configuration is an alternative type of pattern in which region with similar densities cluster together, and results in smaller density differences across each interface.

ry interaction between two interfaces, and of what these basic properties imply for the overall system evolution. Section III contains an analytical calculation of the systems behavior at early times. Section IV is devoted to a direct simulation of the model, and also compares these results with the predictions from Sec. III. Section V contains some concluding remarks concerning diffusion and the applicability of the model to real systems.

II. TWO INTERFACE INTERACTIONS

The model system evolves in time through the movements of the interfaces. Whenever two interfaces meet, a density region disappears, and the density pattern is changed in a fundamental way. It is through a sequence of these two interface collisions that the system moves towards its final state; thus understanding this basic "unit" of the evolution is the first step in understanding the pattern-formation process.

It is worthwhile beginning with a presentation of a mapping of this interface problem to a collision problem from classical mechanics. The interaction of two interfaces involves three density regions, ρ_1, ρ_2, and ρ_3, as shown in Fig. 3. Let the interfaces between regions 1 and 2 and regions 2 and 3 move with velocity v_a and v_b, respectively. Imagine that the densities are such that the interfaces meet and region 2 disappears. The new interface between regions 1 and 3 then moves with velocity v_c. From Eq. (1.2) these velocities can be written as

$$v_a=\frac{j(\rho_1)-j(\rho_2)}{\rho_1-\rho_2},\quad v_b=\frac{j(\rho_2)-j(\rho_3)}{\rho_2-\rho_3},\quad v_c=\frac{j(\rho_1)-j(\rho_3)}{\rho_1-\rho_3}. \tag{2.1}$$

A simple substitution for $j(\rho_1)$ and $j(\rho_3)$ yields the expression

$$(\rho_1-\rho_3)v_c=(\rho_1-\rho_2)v_a+(\rho_2-\rho_3)v_b\ . \tag{2.2}$$

This expression for the final velocity is exactly the equation for the conservation of momentum for a perfectly inelastic collision where the "mass" of each interface is simply the difference in density across the interface. Define the effective mass of an interface, m_i, for each interface as

$$m_i=\rho_i-\rho_{i+1}\ , \tag{2.3}$$

where i indexes each region in the system. Mass conservation in the collision follows from the fact that

$$(\rho_1-\rho_2)+(\rho_2-\rho_3)=(\rho_1-\rho_3)\ . \tag{2.4}$$

However, three things distinguish this particle collision picture from a set of random masses colliding inelastically. First, Eq. (2.3) allows for the existence of particles with negative mass. Second, because neighboring interfaces always share one region in common, there exists some correlation between the masses of neighboring particles. Finally, the curve $j(\rho)$ gives a relationship between the mass of the interface and the velocity. Thus the mass of a particle and its velocity are highly correlated.

In order to continue analysis (beyond just mapping one difficult problem into another one), it is necessary to make some assumptions about the curve $j(\rho)$. For the case of traffic flow this curve is observed to be convex (as in Fig. 4). In the numerical simulations of granular flow in a tube geometry, this curve is also found to be convex. This is equivalent to the condition that the flow velocity is a decreasing function of density.

For the case of convex $j(\rho)$, it is possible to divide all possible two interface configurations into six different categories, as shown in Fig. 5. The classification for a given two-interface configuration is determined by the inequality between the three values for the densities. The first case shown is $\rho_3<\rho_2<\rho_1$. In the following, these different configurations will be referred to as class A-F, with the letter referring to the labeling in the figure.

For three of these configurations, there is a collision, with the middle region being swallowed up by the other two. The three scenarios that result in the destruction of the central region have the common feature that $\rho_1<\rho_3$. Thus for the case of a two-interface interaction, whether or not a particular region survives is not dependent on its density, but on the densities of the regions around it. In the other cases with $\rho_1>\rho_3$, the central region grows in time, and there is no collision.

Also interesting are the implications for typical traffic-jam-creating events. Consider a uniform flow of traffic with density ρ_0. Suddenly, one driver brakes. Thus in front of the car is created a region of low density, and behind a region with slightly higher density. This is shown in Fig. 6. The newly created high-density region (region 2) is a class C configuration; therefore, this region will grow in time. The less dense region (region 3) falls

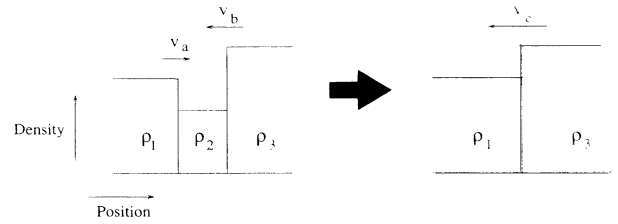

FIG. 3. Basic two-interface collision. State on the left is the initial configuration which evolves to the one shown on the right. The smaller arrows indicate the velocities of the interfaces.

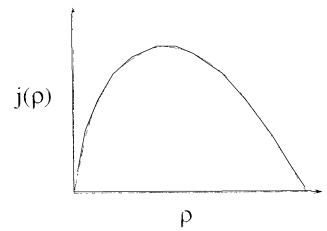

FIG. 4. Typical flux curve. For this curve $j''(\rho)$ is always negative.

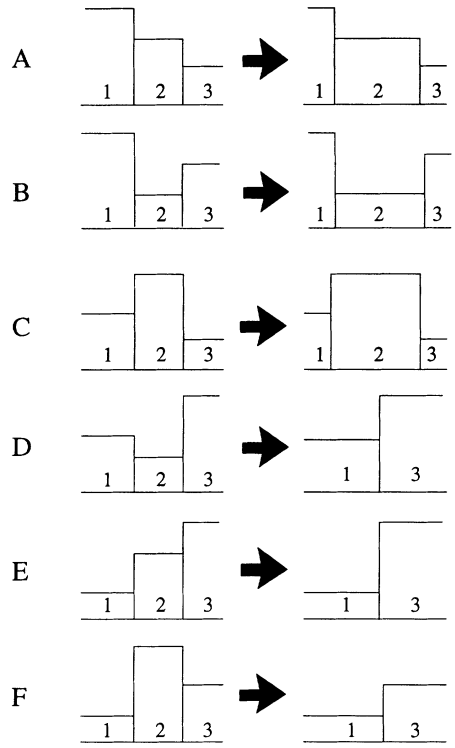

FIG. 5. Fundamental two interface interactions. The configurations on the left evolve in time to the ones on the right. Configurations *A*, *B*, and *C* result in region 2 growing in time, while *D*, *E*, and *F* result in the elimination of region 2.

into class *B*, and this region will also become larger. It is clear that random braking events create regions with contrasting densities.

Consider, conversely, the random acceleration by a driver. Such an event creates a high-density region in front of the automobile, and a less dense region behind, as shown in Fig. 6. In this case, region 2 falls into class *D*, and it will be destroyed in time. Region 3 is a class *F* configuration, and is also engulfed by the regions around it. Thus random accelerations do not affect the large-scale density pattern.

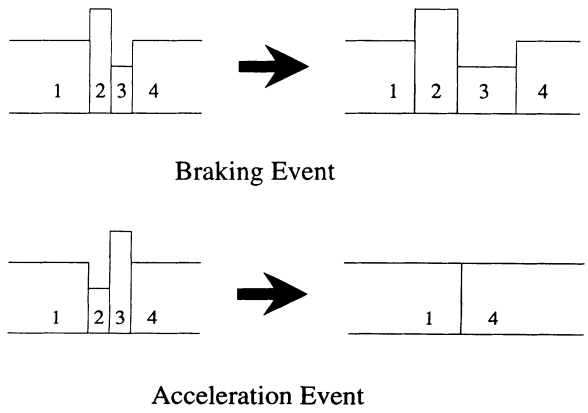

FIG. 6. Density fluctuations in traffic model. The upper picture shows the evolution of the density fluctuations that result from a braking event. The lower picture shows an acceleration event, and the configuration to which it evolves.

Finally, again consider the set of three density regions shown in Fig. 3. Let the length of region 2 be given by l. If $\rho_1 < \rho_3$, then region 2 will disappear when these two interfaces collide, at some time, t. This time is given by

$$t = l/(v_a - v_b) . \tag{2.5}$$

Using Eq. (1.2), this can be written in terms of $j(\rho)$ and the three values for the densities. Consider now an expression of $j(\rho)$ around some ρ_0,

$$j(\rho) = j(\rho_0) + j'(\rho_0)(\rho - \rho_0) + \tfrac{1}{2} j''(\rho_0)(\rho - \rho_0)^2 + O[(\rho - \rho_0)^3] . \tag{2.6}$$

Substituting in this expansion for $j(\rho)$, Eq. (2.5) becomes

$$t \approx \frac{l}{j''(\rho_0)(\rho_1 - \rho_3)/2} , \tag{2.7}$$

where higher-order terms would involve higher-order derivatives of $j(\rho)$. Thus, to first order, the time that it takes for region 2 to disappear is independent of its density. Everything is determined by the density contrast between the two surrounding regions.

For the case of a convex curve, the second derivative $j''(\rho) < 0$, and in order to have a positive collision time from Eq. (2.7), $\rho_1 < \rho_3$. A negative collision time indicates that the interfaces are moving away from each other and no interaction occurs. This is in agreement with the more general result that for *any* convex flux curve a region is destroyed only if $\rho_1 < \rho_3$.

It is also interesting to notice that because in any collision $\rho_1 < \rho_3$, the conversion of two interfaces into one must produce an interface with a negative value for m_i. Therefore, an interface with large positive mass (i.e., a very high-density region, followed by a very low-density region) is very unlikely to be involved in a collision. Such an interface can only collide with an interface which has a larger negative mass.

III. ANALYTIC CALCULATIONS

For early times it is possible to calculate analytically the behavior of this model system. This simplification comes from the fact that there are no correlations between the densities, and one can evaluate statistically which density regions will be destroyed in such a random ensemble. With this approach it is possible to determine macroscopic quantities, such as the total number of interfaces as a function of time, or the time evolution of a quantity averaged over all interfaces, like the average value for $|m_i|$. This latter quantity is of interest because it can serve as an indicator for a state which is primarily made up of interfaces which separate regions with a large density contrast (i.e., a striped pattern).

The calculations presented here can be viewed as the behavior which results if each interface is only permitted to interact once. Thus the results will be accurate at early times when the behavior is dominated by the destruction of the initial fluctuations that were created in very

unfavorable environments and are quickly destroyed. At longer times, however, the behavior of the real system is determined by the interactions of interfaces which result from this first set of collisions. At this time, the predictions from these calculations will be incorrect. However, the trends that emerge are already clear, and these calculations serve to illustrate the type of pattern that interacting kinematic waves produce.

To be explicit, the situation considered here is a collection of N_0 points placed at random on the interval $[0,L]$. These points then become the location of the interfaces. The regions between the interfaces are assigned densities with a uniform distribution in the range $[\rho_0-W,\rho_0+W]$. From this procedure, the probability, $n(l)$, that a single region extends over a length l is given by

$$n(l)=\frac{N_0(N_0-1)}{L}\left[1-\frac{l}{L}\right]^{(N_0-2)} . \tag{3.1}$$

This distribution is normalized so that $\int_0^L n(l)dl=N_0$.

The first quantity calculated is the total number of interfaces as a function of time, $N(t)$. The number of interfaces $dN(t)$ destroyed in a time dt can be written as

$$\frac{dN(t)}{dt}=-\frac{1}{8W^3}\int_{\rho_0-W}^{\rho_0+W}d\rho_1\int_{\rho_0-W}^{\rho_0+W}d\rho_2\int_{\rho_0-W}^{\rho_0+W}d\rho_3\int_0^L dl\,H(\rho_3-\rho_1)\delta\left[t-\frac{l}{K(\rho_3-\rho_1)}\right]n(l) , \tag{3.2}$$

where $H(x)$ is the Heaviside step function, and $K\equiv -j''/2>0$. The integrals are over all possible values of the three densities, and all possible lengths for the density regions. The δ function sets the time for a collision to be that given by Eq. (2.7). The step function ensures that a collision occurs only for $\rho_1<\rho_3$.

Since there is no dependence on ρ_2, this integral is trivial to evaluate. It is possible to use the δ function to remove the integral over l. This essentially exchanges the variable l for $Kt(\rho_3-\rho_1)$. This introduces a finite time cutoff, because for large t, the only interfaces which are destroyed are those whose length l would be longer than the system size L. Equation (3.2) then becomes

$$\frac{dN(t)}{dt}=-\frac{N_0(N_0-1)K}{4W^2L}\int_{\rho_0-W}^{\rho_0+W}d\rho_3\int_{\rho_0-W}^{\rho_3}d\rho_1[1-Kt(\rho_3-\rho_1)/L]^{N_0-2}(\rho_3-\rho_1) , \tag{3.3}$$

where the step function has been incorporated into the limits of the integral over ρ_1. It is easiest to evaluate this integral by expanding the $[1-Kt(\rho_3-\rho_1)]^{N_0-2}$ in a series. The result after some algebra is

$$N(t)-N_0=-\frac{2N_0(N_0-1)KWt}{L}\sum_{i=0}^{N_0-2}\binom{N_0-2}{i}\left[\frac{-2KWt}{L}\right]^i\frac{1}{(i+1)(i+2)(i+3)} . \tag{3.4}$$

Of interest is the behavior as $t\to 0$. In this case (3.4) becomes

$$N(t)-N_0\approx -N_0(N_0-1)KWt/3L . \tag{3.5}$$

This entire series can, of course, be summed numerically, and the results of this will be shown in the next section. It is also worth noting that there is a natural time scale that is suggested by the forms of (3.4) and (3.5), which is $t'=(N_0KW/L)t$ (the necessary factors of N_0 in each term in the series coming from the binomial coefficient).

It is also possible to calculate the time evolution of the average value for $|m_i|$ with this approach. Let

$$M(t)\equiv\sum_{i=0}^{N(t)}|m_i|=\sum_{i=0}^{N(t)}|\rho_i-\rho_{i+1}| . \tag{3.6}$$

The expression for the time derivative of this quantity is

$$\frac{dM(t)}{dt}=\frac{1}{8W^3}\int_{\rho_0-W}^{\rho_0+W}d\rho_1\int_{\rho_0-W}^{\rho_0+W}d\rho_2\int_{\rho_0-W}^{\rho_0+W}d\rho_3\int_0^L dl\,H(\rho_3-\rho_1)\delta\left[t-\frac{l}{K(\rho_3-\rho_1)}\right]$$
$$\times n(l)[|\rho_3-\rho_1|-|\rho_2-\rho_1|-|\rho_3-\rho_2|] , \tag{3.7}$$

which is very similar to Eq. (3.3), with the addition of the term in brackets. This expression is the absolute value of the mass for the new 1-3 interface minus the absolute values of the masses for the now destroyed 1-2 and 2-3 interfaces. Evaluation of Eq. (3.7) proceeds in a way similar to that used in evaluating (3.2), with the final result that

$$M(t)-M_0=-\frac{16N_0(N_0-1)KW^2t}{L}\sum_{i=0}^{N_0-2}\binom{N_0-2}{i}\left[\frac{-2KWt}{L}\right]^i\frac{1}{(i+1)(i+2)(i+3)(i+4)(i+5)} , \tag{3.8}$$

where $M_0 \equiv M(0)$. The value of M_0 can also be calculated analytically, with the result $M_0 = 2N_0 W/3$.

The average value for a single interface $m(t) \equiv M(t)/N(t)$ is simply the ratio of the two series (3.4) and (3.8). Again, it is interesting to look at the $t \to 0$ limit for this quantity,

$$m(t) = 2W/3 + 4(N_0 - 1)KWt^2/45L \ . \tag{3.9}$$

This is probably the most significant result in this section. Equation (3.9) clearly shows that the density contrast at interfaces is becoming sharper in time. If the density pattern were being driven to a more uniform density behavior, then $m(t)$ would decrease in time, and the first correction term would be negative.

IV. NUMERICAL RESULTS

This section presents the results from a direct simulation of a set of density regions driven by the action of kinematic waves. The results confirm the short-time behavior of the two interface calculation and display a power-law behavior in the long-time limit.

The simulation itself is very straightforward. Using a random number generator [8], a series of N_0 values in the range $[0,L]$ are generated to represent the interfaces. Each region between consecutive points is assigned a density value in the range $[\rho_0 - W, \rho_0 + W]$. Once the densities are determined, the velocity of each region can then be calculated.

Periodic boundary conditions are used for simplicity. The simulation itself is event driven. For each pair of consecutive interfaces, the time of collision can be calculated, and all interfaces are then propagated forward to the next collision. The two interfaces which collided are replaced by a new interface and the velocity for this new interface is calculated. This procedure is repeated until the configuration is such that the next collision occurs at $t = \infty$.

Because of the periodic boundary conditions, the only stable configuration is that which has just two density regions. If there are three different density regions, there are then three interfaces traveling at different speeds. Eventually, two of these interfaces will collide, producing a configuration with only two density regions.

The only thing that remains is the choice of flux curves $j(\rho)$. The simplest possible curve that satisfies the convexity condition is

$$j(\rho) = J_0 \frac{\rho}{R}(1 - \rho_R) \ , \tag{4.1}$$

where R is the maximum density for the system, and J_0 is one quarter of the maximum throughout of the system. For this curve, the constant $K = J_0/R^2$. Note that for a flux curve of the form (4.1), Eq. (2.7) becomes exactly true.

While a system may have a much more complicated flux curve than (4.1), this form can be taken as the approximate curve around an average density ρ_0. In this case, J_0 and R are fitting parameters, and the analysis using the simple parabolic form will hold as long as $W/\rho_0 \ll 1$. For the simulations presented here, $J_0 = R = 1$.

Figure 7 shows the density evolution from an initial set of 200 interfaces, with densities chosen in the range of [0.3:0.8]. The gray scale indicates the density of the region, black being $\rho = 1$, white signifying $\rho = 0$. It is clear from the picture that there is a large density contrast in the final state. The high-density region has $\rho = 0.793$, and the low-density region has $\rho = 0.319$.

This feature, that the densities of the two regions in the final state are near to the extremal values, is found in all simulations, independent of the values for the ρ_0 or W. The surviving regions are not the largest or the smallest that existed at $t = 0$, but are very near the extremes. This can be understood by a simple argument. Consider the interface which separates a region which has a density very near the maximum, followed by a region near the lowest allowed density. This interface has a very large positive mass, and thus is very unlikely to collide with its nearby interfaces. In the long-time limit, this is the type of interface that can expected to live for a long time.

Figure 8 shows the early time behavior for systems with 1000, 10 000, and 100 000 interface. The values for (ρ_0, W) were (0.3,0.1), (0.6,0.3), and (0.8,0.2), respectively. The x axis shows the rescaled time $t' = (N_0 KW)t$, as suggested by the analytical calculations, while the y axis shows the fraction of the initial interfaces that have been destroyed. The simulation for $N_0 = 100\,000$ was only propagated up to the time where $N(t) = 99\,000$.

Also shown in the figure is the results from a direct summation of the series (3.4). The agreement at short

FIG. 7. Density pattern in model system. Gray scale indicates density of region, with darker regions representing higher densities. Position along the interval is the y axis, and time is the x axis. Positive flux is in the $+y$ direction. Thus, while the pattern moves downward, the material actually is moving upward.

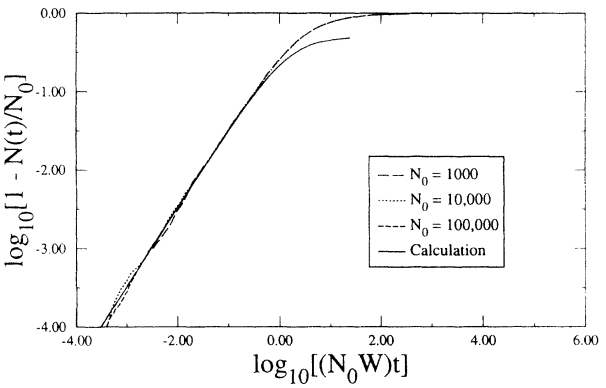

FIG. 8. Fraction of interfaces destroyed as a function of time. The x axis is a rescaled time. The solid line shows the results from directly resuming the series from the two-interface calculations.

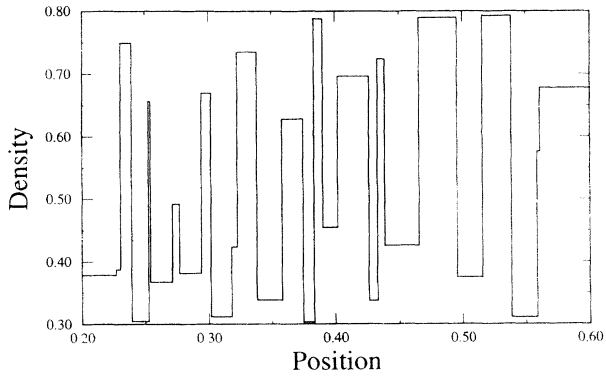

FIG. 10. Density as a function of position along the interval. The curve is taken from Fig. 7, and at this point in the simulation 72 of the original 200 interfaces remain.

times is clearly seen. However, as the fraction of interfaces destroyed becomes larger, there is a significant deviation. The analytical result levels out when one-half of the interfaces have been destroyed. This is to be expected for a calculation in which each interface is only allowed to interact one time. Consider the region of density ρ_2 in a system of three regions and two interfaces. This region will disappear only if $\rho_1 < \rho_3$. With a random collection of densities, this condition should be satisfied for one-half of all configurations. Thus allowing only one iteration of this region swallowing process means that one-half of all of the density regions disappear and only one-half of the original interfaces remain.

Figure 9 shows the value of $[m(t)-m_0]$ as a function of time [where $m_0 \equiv m(0)$]. Again the time has been rescaled, and the $[m(t)-m_0]$ axis has been rescaled by the value of W. Also shown in the figure are the results from the summation of the series expression for $m(t)$. Again, the short-time agreement is excellent. As in the case for the number of interfaces, at long times, the two interface calculation does not reproduce the correct behavior.

The turning down of the curve from the series summation is also to be expected. From (2.7), it is clear that collisions which occur at very late times are those that have a very small value for $\rho_1-\rho_3$. The resulting interfaces that are created at late times have very small values of $m_i=\rho_1-\rho_3$. The two interfaces which were destroyed to create this new interface would have had, on average, larger values for m_i. Thus the average value of m_i for all interfaces decreases as a result of these late-time collisions.

The increase at short times in $m(t)$ indicates that the system is evolving toward a stripe-type pattern with very large density contrasts at each interface. The final value for $m(t) \approx 2W$, which is what is expected if most of the interfaces are showing density contrasts as large as the largest contrast available from the initial noise distribution. A picture of the density regions at $N(t)/N_0 = 0.36$ is shown in Fig. 10. The system has clearly evolved to a stripe pattern.

The evolution from this stripe state to the final two-region configuration is also very interesting. A plot that illustrates the long-time evolution is shown in Fig. 11. The fraction of interfaces remaining is plotted as a function of the rescaled time. For the case of 10 000 initial interfaces, a power-law region can be seen over three decades in time. The exponent for the power law is

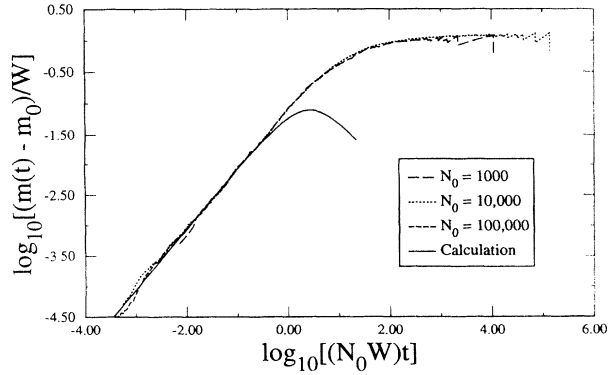

FIG. 9. Average value of $m(t)$ as a function of time. The x axis is a rescaled time. The solid line is the result from a direct summation of the two-interface calculation.

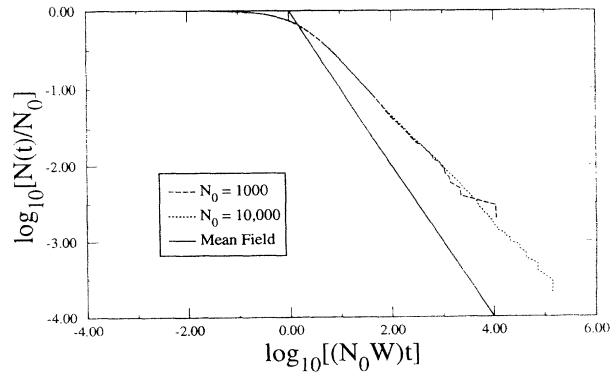

FIG. 11. Fraction of remaining interfaces as a function of time. The x axis is a rescaled time. The solid line shows the behavior predicted by the mean-field theory at long times.

$\approx -2/3$.

The simplest theory of this long-time behavior involves a mean-field-type argument. On general grounds, the change in the number of interfaces as a function of time might be expected to go as

$$\frac{dN(t)}{dt} \approx -\frac{n}{\tau} , \tag{4.2}$$

where τ is the time scale for a collision to occur. The expected form for $\tau \approx l/\Delta v$, where $l \approx 1/N(t)$ is the typical length between interfaces, and Δv is the velocity difference between two consecutive interfaces. If Δv is approximately a constant, then (4.2) becomes

$$\frac{dN(t)}{dt} \approx -n^2 \Delta v . \tag{4.3}$$

This has the long-time solution

$$N(t) \sim t^{-1} . \tag{4.4}$$

This is the wrong exponent, indicating that the correlations from the stripe pattern are important in determining the long-time behavior of the system.

V. CONCLUSIONS AND DISCUSSION

The purpose of this paper is to show that the formation of the density patterns apparent in granular systems and traffic jams can be understood within the formalism of kinematic wave theory. A random pattern due to the noise in the system is organized into a set of macroscopic density regions with large density contrasts. Analytic calculation of the early-time behavior agrees well with the results from numerical simulations. The long-time behavior exhibits an anomalous power-law region.

The major fault with the approach taken here is that the diffusion process that must occur across an interface which separates regions with different densities has been totally ignored. This diffusion effect will cause the fronts to spread out and become less sharp in time. Part of this effect is already present in the kinematic wave formalism itself [7], and will be discussed here. Consider the case of linear fronts, instead of perfectly sharp interfaces, as shown in Fig. 12. Within the kinematic wave approach, it can be shown that the system will evolve a well-defined shock behind the density fluctuation. However, the leading edge will spread out in time, as indicated in the figure. For a parabolic flux curve, the linear form for the front of the wave will be preserved. The time, T, at which the point B reaches point A is given by

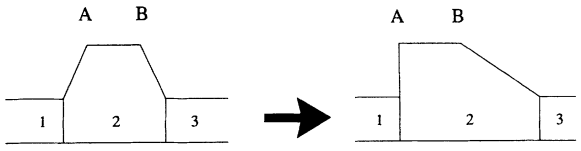

FIG. 12. Density fluctuation with linear density fronts rather than sharp interfaces. Under the evolution of the kinetic wave theory, the interface at A becomes sharper, while the interface at B diffuses in time.

$$T \approx l/K(\rho_1 - \rho_0) , \tag{5.1}$$

where l is the initial distance between points A and B. This time is of the same order as the time for a typical interface collision driven by the density contrast $\rho_1 - \rho_0$. Thus this diffusion effect is relevant, and neglecting it has probably left out some of the physics. However, this diffusion effect does not completely dominate the system either. The reality is probably somewhere in between, and the work presented here is a first attempt to examine interacting density fluctuations within the kinematic wave approach. There certainly is other work to be done.

ACKNOWLEDGMENTS

I would like to thank Jysoo Lee for helpful discussion and guidance during the course of this research. Many hours of useful and stimulating conversations were had with Kai Nagel and Hans Hermann. Finally, I would like to thank Stephan Melin, Greg Kohring, Renaud Delannay, Nobuyasu Ito, and Christian Moukarzel for helpful discussion.

[1] T. Musha and H. Higuchi, Jpn. J. Appl. Phys. **17**, 811 (1978); O. Biham, A. A. Middleton, and D. Levine, Phys. Rev. A **46**, R6124 (1992); J. A. Cuesta, F. C. Martinez, J. M. Molera, and A. Sánchez, University of Carlos III de Madrid Report No. MA/UC2M/4/93 (unpublished).

[2] K. Nagel and M. Schreckenberg, J. Phys. (France) **2**, 2221 (1992).

[3] T. Pöschel, HLRZ Report No. 67/92 (unpublished).

[4] J. O. Cutress and R. F. Pulfer, *Powder Technol.* **1**, 213 (1967); G. W. Baxter, B. P. Behringer, T. Fagaert, and G. A. Johnson, Phys. Rev. Lett. **62**, 2825 (1989).

[5] G. Ristow and H. J. Herrmann, HLRZ Report No. 2/93 (unpublished).

[6] J. Lee, this issue, Phys. Rev. E **49**, 281 (1994).

[7] M. J. Lighthill and G. B. Whitham, Proc. R. Soc. London, Ser. A **229**, 281; M. J. Lighthill and G. B. Whitham, Proc. R. Soc. London, Ser. A **229**, 317.

[8] W. Press, B. Flannery, S. Teukolsky, and W. Vetterling, *Numerical Recipes: The Art of Scientific Computing* (Cambridge University Press, New York, 1988).

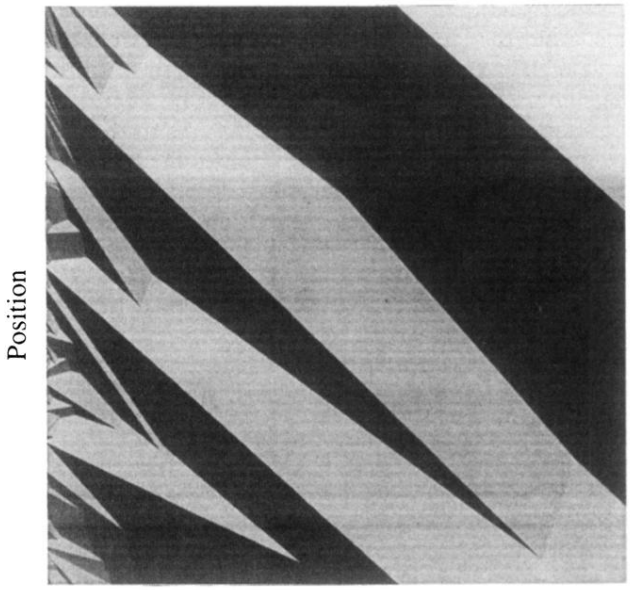

FIG. 7. Density pattern in model system. Gray scale indicates density of region, with darker regions representing higher densities. Position along the interval is the y axis, and time is the x axis. Positive flux is in the $+y$ direction. Thus, while the pattern moves downward, the material actually is moving upward.